

**Zeitschrift:** IABSE reports of the working commissions = Rapports des commissions de travail AIPC = IVBH Berichte der Arbeitskommissionen

**Band:** 34 (1981)

**Artikel:** Analytical model for deformed bar bond under generalized excitations

**Autor:** Ciampi, V. / Eligehausen, R. / Bertero, V.

**DOI:** <https://doi.org/10.5169/seals-26879>

### **Nutzungsbedingungen**

Die ETH-Bibliothek ist die Anbieterin der digitalisierten Zeitschriften. Sie besitzt keine Urheberrechte an den Zeitschriften und ist nicht verantwortlich für deren Inhalte. Die Rechte liegen in der Regel bei den Herausgebern beziehungsweise den externen Rechteinhabern. [Siehe Rechtliche Hinweise.](#)

### **Conditions d'utilisation**

L'ETH Library est le fournisseur des revues numérisées. Elle ne détient aucun droit d'auteur sur les revues et n'est pas responsable de leur contenu. En règle générale, les droits sont détenus par les éditeurs ou les détenteurs de droits externes. [Voir Informations légales.](#)

### **Terms of use**

The ETH Library is the provider of the digitised journals. It does not own any copyrights to the journals and is not responsible for their content. The rights usually lie with the publishers or the external rights holders. [See Legal notice.](#)

**Download PDF:** 17.11.2024

**ETH-Bibliothek Zürich, E-Periodica, <https://www.e-periodica.ch>**

## **Analytical Model for Deformed Bar Bond under Generalized Excitations**

Modèle analytique pour l'adhérence de barres nervurées sous sollicitations répétées

Analytisches Modell für den Verbund von Rippenstählen unter beliebigen Beanspruchungen

**V. CIAMPI, R. ELIGEHAUSEN**

Visiting scholars  
University of California  
Berkeley, USA

**V. BERTERO, E. POPOV**

Professor  
University of California  
Berkeley, USA

### **SUMMARY**

A mathematical model is presented to predict the behavior of a deformed bar, embedded in well-confined concrete, and subjected to generalized cyclic excitations in the range of the low cycle fatigue. It includes the formulation of a simplified model for the local bond stress-slip relationship, based on the elaboration of the result of an extensive experimental study carried out recently at Berkeley; use of a simple but sufficiently accurate model for the stress-strain relationship of reinforcing steel and the numerical solution of the differential equation of bond. An example is presented and commented.

### **RÉSUMÉ**

Un modèle mathématique décrivant le comportement d'une barre crénelée dans un béton bien confiné et soumis à un chargement cyclique quelconque de haute intensité est présenté. Il comprend: 1) la formulation d'un modèle simplifié pour décrire la relation contrainte-glissement en adhérence basé sur les résultats d'un vaste programme expérimental mené récemment à Berkeley, 2) l'utilisation d'un modèle simple mais suffisamment exact pour décrire la relation contrainte-déformation dans la barre d'armature et 3) une solution numérique de l'équation différentielle décrivant l'adhérence. Un exemple est présenté et commenté.

### **ZUSAMMENFASSUNG**

Ein mathematisches Modell zur Berechnung des Verhaltens eines Rippenstabes, verankert in eng verbügeltem Beton und beansprucht durch beliebige zyklische Belastungen hoher Intensität, wird erläutert. Es umfasst die Formulierung eines vereinfachten Modells für die Beziehung zwischen örtlicher Verbundspannung und örtlichem Schlupf, das aus umfangreichen, in Berkeley durchgeführten Versuchen abgeleitet wurde; die Benutzung eines einfachen, jedoch ausreichend genauen Modells für das Spannungs-Dehnungs Gesetz des Bewehrungsstahles und die numerische Lösung der Differentialgleichung des Verbundes. Ein Beispiel ist dargestellt und erläutert.



## 1. INTRODUCTION

Under severe seismic excitations, the hysteretic behavior of reinforced concrete structures is highly dependent on the interaction between steel and concrete (bond stress-slip relationship) [1]. Tests show that developing displacement ductility ratios of four or more, fixed end rotations caused by slip of the main steel bars along their embedment length in beam-column joints, may contribute up to 50 percent of the total beam deflections [2-4]. These effects must be included in the analyses. However, in spite of recent integrated experimental and analytical studies devoted to finding such a relationship [5], no reliable bond stress-slip laws for generalized excitations are available [6].

In this paper a mathematical model is presented to predict the behavior of a deformed bar, embedded in well-confined concrete, and subjected to generalized cyclic excitations. The local bond stress-slip model, the model for the stress-strain relationship of reinforcing steel, and the technique for solving the differential equation of bond, are discussed and an example is presented.

## 2. LOCAL BOND STRESS-SLIP MODEL

### 2.1 Tests

The constitutive relations for bond between deformed bars and normal weight concrete were derived from results of an extensive experimental study carried out at Berkeley during the last year [7]. Altogether some 120 specimens were tested; only those results which are relevant to the formulation of the proposed analytical model are briefly discussed herein.

The test specimens (Fig. 1) represented the confined region of a beam-column joint. Only a short length ( $5d_b$ ) of a grade 60 deformed bar (#8,  $d_b \sim 25$  mm) was embedded in concrete ( $f'_c = 30$  N/mm<sup>2</sup>). Because cracking might influence the bond stress-slip behavior, the resistance against splitting was simulated as closely as possible to that which might exist in a real structure. Therefore a thin plastic sheet was placed in the plane of the longitudinal axis of the bar (Fig. 1) which limited the concrete splitting area to the desired value. In

Fig. 1 Test Specimen

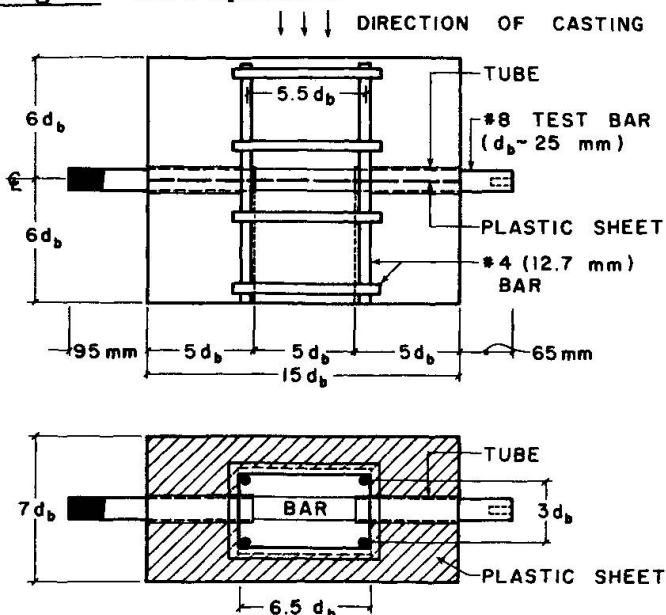


Fig. 2 Foto illustrating test setup

this way the influence of different bar spacings could be modeled as well. In the tests described here, the assumed spacing was  $4 d_b$ . The test specimen was installed in a specially designed testing frame (Fig. 2) and was loaded by a hydraulic servo controlled universal testing machine having a capacity  $\pm 1350$  kN, which allowed the application of prescribed tension and compression forces, or displacements, to the embedded bars. The tests were run under displacement control by subjecting the threaded loading end of the bar to the required force needed to induce the desired slip, which was measured at the unloaded bar end (using a linear variable differential transformer, (Fig. 2) and was controlled at a rate of 1.7 mm/min.

The influence of various slip histories on the bond stress-slip behavior was examined. The main parameters were: the peak value of the slip ( $0.1 \text{ mm} \leq s_{\max} \leq 15 \text{ mm}$ ); the difference between the peak values of slip ( $\Delta s = s_{\max} - s_{\min}$ , see Fig. 3a) between which the specimen was cyclically loaded ( $\Delta s = 0.05 \text{ mm}$ ,  $1 s_{\max}$  and  $2 s_{\max}$ ); and the number of cycles (1 to 10). In the majority of tests, after the specimens were subjected either to 1 or alternatively to 10 cycles up to the selected peak values of slip, the slip was increased monotonically to failure. In a few tests the bar was subjected to a series of cycles at different values of slip. Usually 2 or 3 identical tests were carried out.

In all tests conducted the failures were caused by pulling out of the bars at steel stresses well below yield stress. Prior to failure, splitting cracks developed in the plane of the longitudinal axis of the bars but their growth was controlled by the confining reinforcement (see Fig. 1).

Typical test results are shown in Fig. 3 and summarized below:

- (a) The bond stress-slip relationship for monotonic loading in tension was almost identical to that in compression. This could be expected [8] since the specimens were cast with the bars in a horizontal position. The descending branch of the bond stress-slip curve levelled off at a slip approximately equal to the clear distance between protruding lugs of the bar.
- (b) If the peak bond stress in tension and compression during cycling did not exceed 70-80 percent of the monotonic  $\tau_{\max}$ , the ensuing bond stress-slip relationship, at slip values larger than the one at which the specimen was cycled, was not significantly affected by up to 10 cycles (Fig. 3a). The bond stress at peak slip deteriorated moderately with increasing number of cycles. These results agree well with earlier findings [9-12]. Although many factors related to early concrete damage (microcracking and microcrushing due to high local stresses at the protruding lugs) may be involved in this bond-resistance deterioration it is believed that the main cause is a relaxation of the concrete between the lugs [12].
- (c) When the bar was loaded monotonically to an arbitrary slip value and then cycled up to 10 times between this slip value and a slip value corresponding to a load equal to zero ( $\Delta s = 0.05 \text{ mm}$ ), the monotonic envelope was, for all practical purposes, reached again. From then on the behavior was the same as that obtained in a monotonic test. This agrees well with earlier results [8,11].
- (d) Loading to slip values inducing a  $\tau$  larger than 80 percent of the monotonically obtained  $\tau_{\max}$  in either direction led to a degradation in the bond stress-slip behavior in the reversed direction (Figs. 3b and 3c). The bond stress-slip relationship at slip values larger than the peak value during previous cycles, with  $\Delta s = s_{\max}$  or  $\Delta s = 2 s_{\max}$ , was significantly different from the virgin monotonic envelope. There was a deterioration of the bond resistance and the degree of deterioration increased with increasing peak slip  $s_{\max}$ , increasing  $\Delta s$ , and increasing number of cycles (Fig. 3b and 3c). The largest deterioration was observed for full reversals of slip ( $\Delta s = 2 s_{\max}$ ).

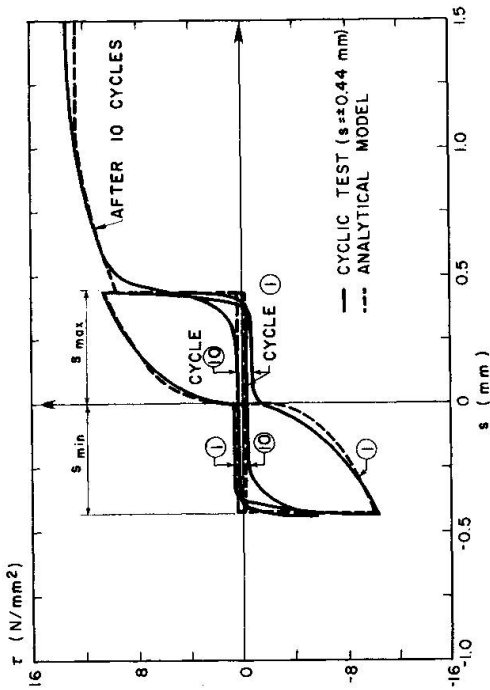


Fig. 3a Cycling between  $s = \pm 0.44$  mm

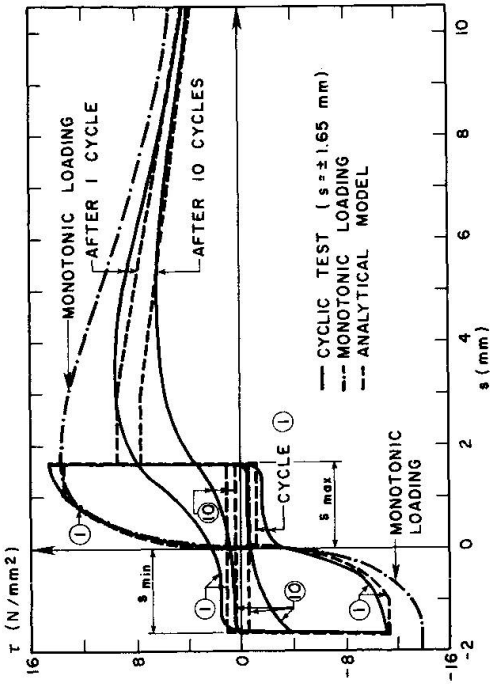


Fig. 3b Cycling between  $s = \pm 1.65$  mm

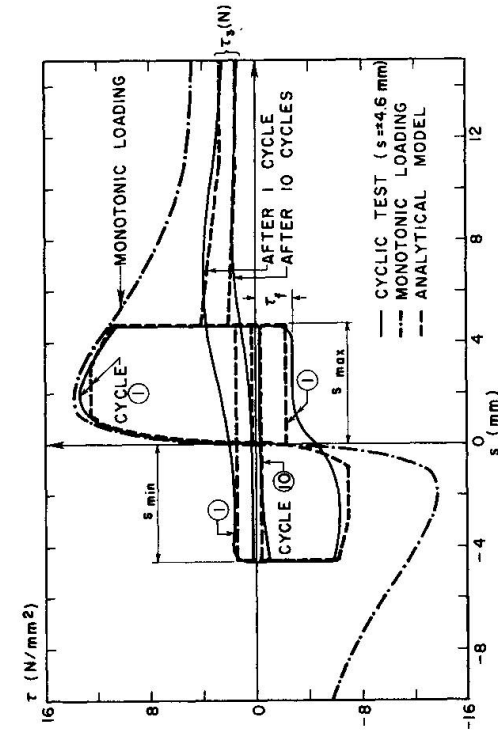


Fig. 3c Cycling between  $s = \pm 4.6$  mm

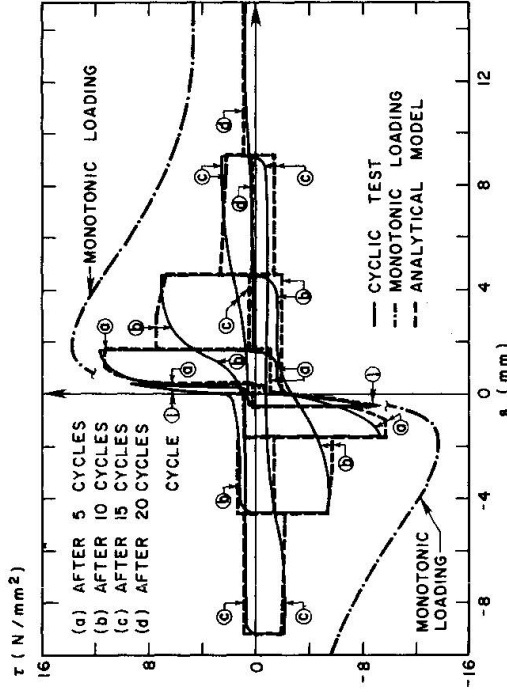


Fig. 3d Cycling under different increasing  $s_{max}$

Fig 3 Comparison of Experimental and Analytical Results on Local Bond Stress-Slip Relationship.

The observed behavior can be explained by assuming that in a well-confined reinforced concrete the maximum bond resistance is controlled by the initiation of a shear failure in a part of the concrete between the protruding lugs of the bar. The larger is the value of the slip with respect to  $s_{\tau_{max}}$ , i.e. slip at  $\tau_{max}$ , the larger is the area of concrete between the lugs that is affected by the shear failure, and the smaller is the bond resistance. If the bar is cycled between constant peak values of  $s_{max}$  and  $s_{min}$ , the main damage is done in the first cycle. During successive cycles, the concrete at the cylindrical surface where shear failure occurred, is mainly grounded off, decreasing its interlocking and frictional resistance.

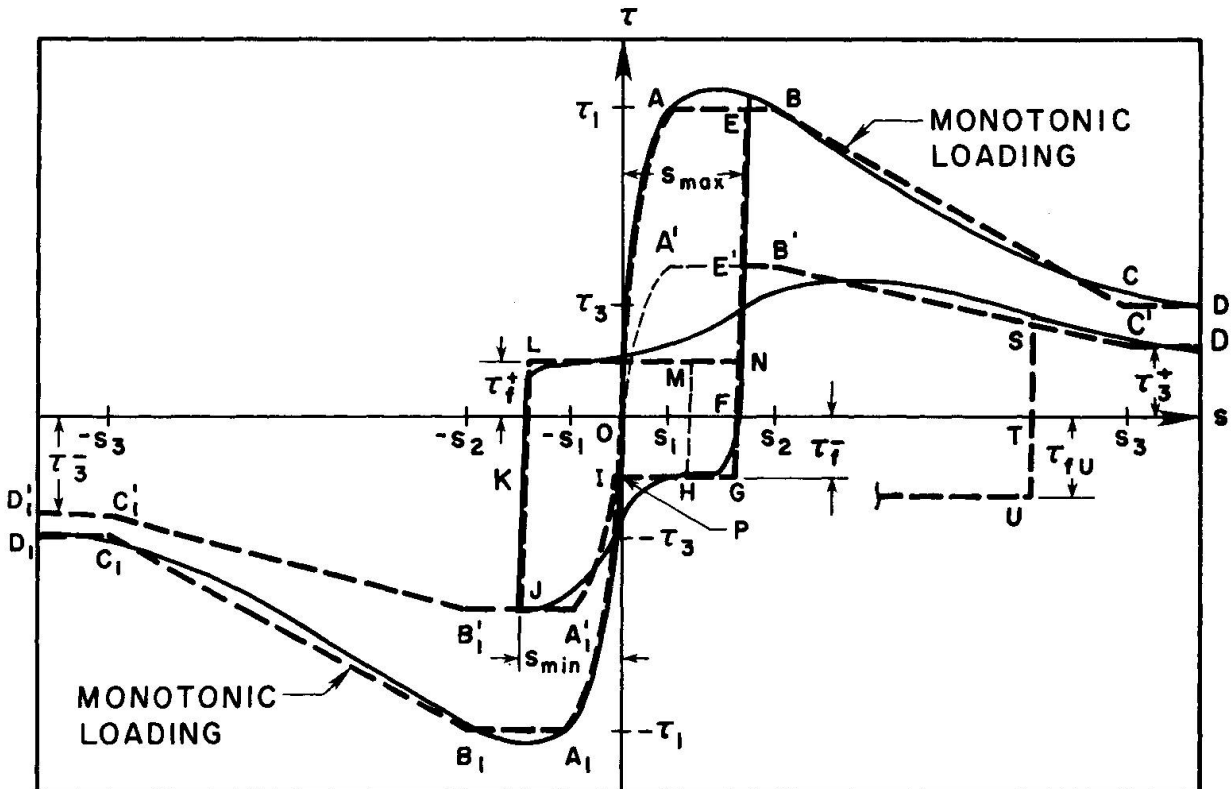
(e) The frictional bond resistance,  $\tau_f$ , during cycling was dependent upon the value of the peak slip  $s_{max}$ . With repeated cycles  $\tau_f$  deteriorated rapidly (see Figs. 3a-d), approximately at the same rate as the bond resistance at the peak slip value  $s_{max}$ , but at a faster rate than the ultimate frictional bond resistance  $\tau_3(N)$  (see Fig. 3c) of the corresponding reduced envelope curve. The mechanism and value of frictional bond resistance are not well described and predicted by existing proposals [6].

2.2 Analytical Local Bond Stress-Slip Model

The assumed bond model is illustrated in Fig. 4. Although it simplifies the observed real behavior, it takes into account the significant parameters that appear to control the behavior observed in the experiments. This model, in spite of being simpler than the one proposed in [5], is believed to be more general. The model's main characteristics, illustrated by following a typical cycle (Fig. 4), are described below.

When loading the first time, the assumed bond stress-slip relationship follows a curve valid for monotonically increasing slip, which is called herein "monotonic envelope" (paths OABCD or  $OA_1B_1C_1D_1$ ). Imposing a slip reversal at an

Fig. 4 Proposed Analytical Model for Local Bond Stress-Slip Relationship.





arbitrary slip value, a stiff "unloading branch" is followed up to the point where the frictional bond resistance  $\tau_f$  is reached (path EFG). Further slip-page in negative direction takes place without increase in  $\tau$  up to the intersection of the "friction branch" with the curve  $OA'_1$  (path GHI). If more slip in negative direction is imposed a bond stress-slip relationship similar to the virgin monotonic curve is followed, but with values of  $\tau$  reduced as illustrated by the paths  $IA'_1J$ . This curve ( $OA'_1B'_1C'_1D'_1$ ) is called "reduced envelope". When reversing the slip again at J, first the unloading branch and then the frictional branch with  $\tau = \tau_f^+$  are followed up to point N, which lies on the unloading branch EFG (path JLN). At N the "reloading branch" (same stiffness as the unloading branch) is followed up to the intersection with the reduced envelope  $OA'B'C'D'$  (path NE'), which is followed thereafter (path E'B'S). If instead of increasing the slip beyond point N more cycles between the slip values corresponding to the points N and K are imposed, the bond stress-slip relationship is like that of a rigid plastic model, the only difference being that frictional bond resistance decreases with increasing number of cycles. A similar behavior as described is followed if the slip is reversed again at point S (path STU). To complete the illustration of the model details about the different branches referred to in the above overall description are given in the following.

#### a) Monotonic Envelope

The simplified monotonic envelope simulates the experimentally obtained curve under monotonically increasing slip. It consists of an initial nonlinear relationship  $\tau = \tau_1 (s/s_1)^\alpha$  valid for  $s \leq s_1$ , followed by a plateau  $\tau = \tau_1$  for  $s_1 \leq s \leq s_2$ . For  $s \geq s_2$ ,  $\tau$  decreases linearly to the value of the ultimate frictional bond resistance  $\tau_3$  at a slip value of  $s_3$ . This value  $s_3$  is assumed to be equal to the clear distance between the lugs of the deformed bars. The same bond stress-slip law is assumed regardless of whether the bar is pulled or pushed.

At present, the values  $s_1, s_2, \tau_1, \tau_3$  and  $\alpha$  are chosen to match the experimentally obtained monotonic envelope curve. Studies are in progress to formulate reliable rules to predict such a curve for conditions different from those in the tests.

#### b) Reduced envelopes

Reduced envelopes are obtained from the monotonic envelope by reducing the characteristic bond stresses  $\tau_1$  and  $\tau_3$  through reduction factors, which are formulated as a function of one parameter, called herein the "damage parameter  $d$ ". For no damage,  $d=0$ , the reloading branch reaches the monotonic envelope. For full damage,  $d=1$ , bond is completely destroyed ( $\tau = 0$ ).

The rationale for this assumption is given by Fig. 5, which shows that reloading curves for similar specimens, subjected to different loading histories, appear to form a parametric family of curves.

The deterioration of the monotonic envelope seems to depend on the damage experienced by the concrete, particularly the length of the concrete between the lugs of the bar that has sheared off. This in turn is a function of the magnitude of the slip induced in the bar in both directions, the larger the  $s_{max}$  and the difference between peak slip values, the larger the damage. Another influence factor is the number of cycles. These parameters can be related to the energy dissipated during the loading and unloading processes. Therefore it was assumed that the damage parameter  $d$  is a function of the total dissipated energy only. However, it has also been taken into account that only a fraction of the energy

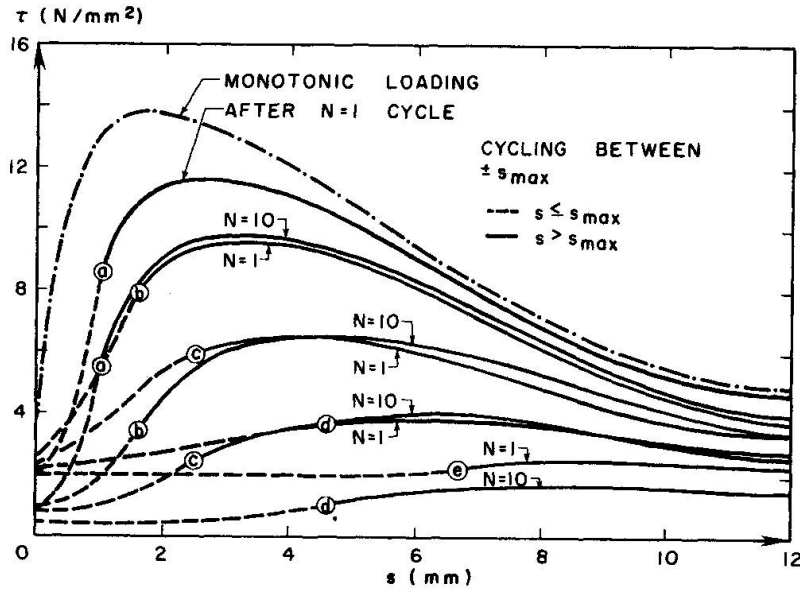


Fig. 5 Effects of number of cycles and of the peak values of slip  $s_{max}$  at which the cycling is performed on the ensuing bond stress-slip relationship for  $s > s_{max}$ .

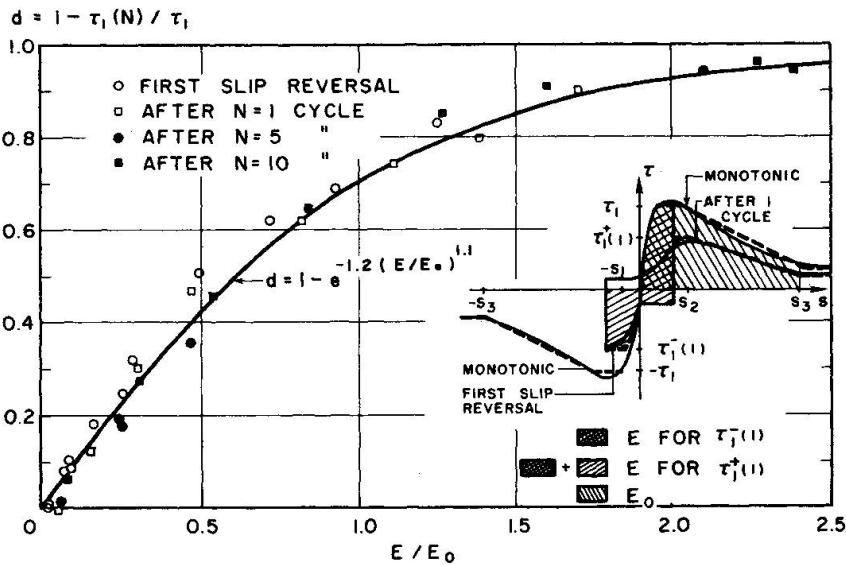


Fig. 6 Damage parameter  $d$  as a function of the dimensionless energy dissipation.

dissipated during subsequent cycles between fixed peak slip values appear to cause damage, while the other part appears to be used to overcome the frictional resistance and is transformed into heat.

Fig. 6 illustrates the correlation between the measured damage factor  $d$ , for tests with full reversal of slip as a function of the computed dimensionless dissipated energy factor  $E/E_0$ . The proposed function for  $d$  is shown as well. In the computation of  $E$  only 50% of the energy dissipated by friction is taken into account. The normalizing energy  $E_0$  corresponds to the absorbed energy under monotonically increasing slip up to the value  $s_3$ . Although there is some scatter, the agreement between the analytical and experimental results seems acceptable.





No reduction of the current envelope (monotonic or reduced) is assumed for unloading and reloading only (e.g., paths EGE or JLJ in Fig. 4). If a cycle is not completed to the current values of  $s_{max}$  or  $s_{min}$  (e.g., path GHM) the damage parameter is interpolated between the values valid for the last slip reversal and for the completed cycle (point E and point P in this example).

It should be observed that the proposal for calculating the damage parameter as a function of the total dissipated energy is theoretically correct only in the range of the low cycle fatigue, that is when a small number of cycles at relatively large slip values is carried out. In fact if a high number of cycles at small slip values is performed, the energy dissipated can be relatively large but no significant damage is produced and the reloading branch reaches the monotonic envelope again [12]. On the other hand, when limiting our attention to a small number of cycles ( $< 30$ ), as in the present study, the energy dissipated for cycles between small slip values is rather small and the calculated damage, as a consequence, insignificant.

### c) Frictional resistance

The frictional bond resistance after first unloading ( $\tau_f^-$  in Fig. 4) depends upon the peak value of slip,  $s_{max}$ , and is related to the value of the ultimate frictional bond resistance of the corresponding reduced envelope ( $\tau_3^-$  in Fig. 4). The relationship found in the tests is shown in Fig. 7. However, if cycling is done between fixed values of slip (e.g., between  $s_{max}$  and  $s_{min}$  in Fig. 4),  $\tau_f$  is reduced more rapidly than the ultimate  $\tau_3$  of the corresponding reduced envelope (see Figs. 3 and 7). Therefore the analytical function oabc in Fig. 7 is used only for the calculation of the frictional resistance for the first slip reversal. For subsequent cycles  $\tau_f$  (e.g.,  $\tau_f^+$  in Fig. 4) is deduced from this initial value by multiplying it with an additional reduction factor which depends on the energy dissipated by friction alone.

If unloading is done from a larger slip value than the peak slip in the previous cycle (path STU) the new frictional bond resistance ( $\tau_{fU}$ ) is interpolated between two values. The first value is related to  $\tau_3^-$  of the corresponding new reduced envelope using the analytical function given in Fig. 7 and the second value is the  $\tau_f$  reached in the last cycle ( $\tau_f^+$  in Fig. 4). This interpolation is done in order to have a smooth transition in the values of  $\tau_f$ .

Note that the concept of relating damage to one scalar quantity, like the normalized dissipated energy, has provided a basis for the relatively easy generalization of the bond behavior for random excitations. The bond model selected can easily be extended to cover bond of bars under conditions different from those reported herein, such as different bar diameter, pattern of deformation (lugs), concrete strength, degree of confinement, effect of transverse pressure, etc. This requires that the pertinent experimental data necessary for computing the different parameters, in particular the monotonic envelope, be obtained.

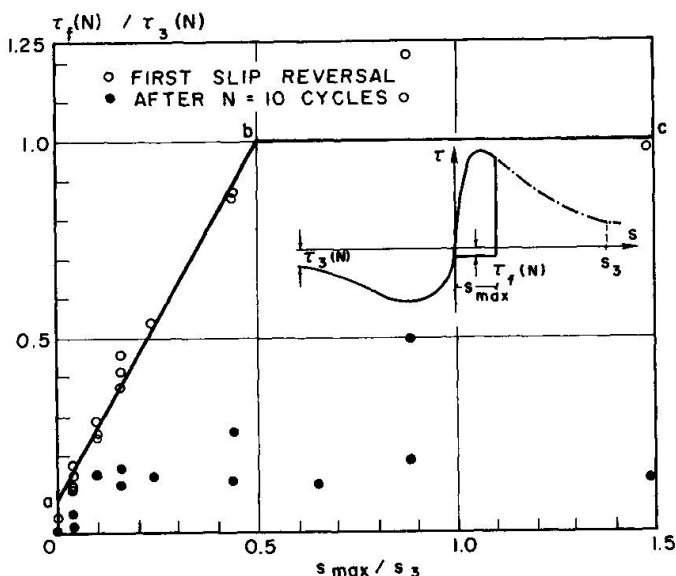


Fig. 7 Relationship between the frictional bond resistance  $\tau_f(N)$  and the corresponding ultimate frictional bond resistance  $\tau_3(N)$ .

### 2.3 Comparison of Analytical Predictions of Local Bond Stress-Slip Relationships with Experimental Results

The local bond stress-slip relationships, obtained using the model described above, are compared in Fig. 3 with the experimental results obtained in some of the Berkeley tests. As can be seen, except for the reloading curves near the values of the peak slip between which the specimen was cycled, the agreement is quite good. In general the model was successful in reproducing most of the experimental results.

### 3. APPLICATION OF LOCAL BOND STRESS-SLIP MODEL IN PREDICTING BOND BEHAVIOR OF REINFORCING BARS

As noted in the introduction, prediction of response of concrete structures to severe seismic excitations requires the prediction of the slippage of the main longitudinal reinforcing bars in their joints. The above formulation of the local bond stress-slip relationship for well-confined concrete allows determination of slippage of the bar in the part of concrete that is well-confined. This is discussed in Chapter 3.2. Since, in general, the anchorage offered to the bars is sufficient to develop the yield strength of the reinforcing steel, it is necessary to have a reliable mechanical model for reinforcing steel covering its inelastic behavior.

#### 3.1 Reinforcing Steel Model

For the uniaxial  $\sigma$ - $\epsilon$  relationship of the reinforcing steel, the expression proposed in [13] and generalized in [14] was used because of its advantages in the present application with respect to the classic Ramberg-Osgood formulation, that has been used in [4,5]. The equation

$$\frac{\sigma}{\sigma_0} = b \frac{\epsilon}{\epsilon_0} + \frac{(1-b) \epsilon/\epsilon_0}{[1 + (\epsilon/\epsilon_0)^R]^{1/R}}$$

where  $\sigma_0$ ,  $\epsilon_0$  are the stress and strain at first yielding respectively, expresses stress  $\sigma$  as a function of strain  $\epsilon$  and accounts for strain hardening through the slope parameter  $b$ . It also allows an accurate representation of the reversal curves through the parameter  $R$ , which varies depending on the magnitude of the maximum excursion  $\epsilon_{\max}$  into the plastic range (see Fig. 8).

The simple set of additional rules proposed in [15] was used to avoid the storage of parameters of all reversal curves in the case of a general strain history. Using a proper set of numerical values for the parameters describing the model, the calculated response of a reinforcing bar subjected to a

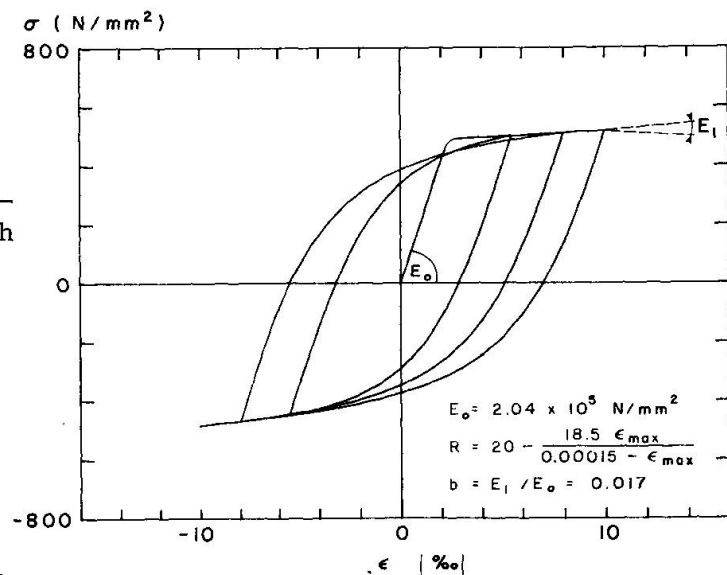


**Fig. 8** Analytically predicted uniaxial stress-strain relationship for a #8 Grade 60 reinforcing steel bar.



particular history of strains, Fig. 8, agrees sufficiently well with test results published in [5].

### 3.2 Technique for Solving the Differential Equation of Bond

The actual behavior of a bar of finite length embedded in a concrete block can be idealized as a one-dimensional problem and modeled using the ordinary nonlinear differential equation

$$dN(x)/dx + q(x) = 0 \quad \text{where } q(x) = \pi d_p \tau(x) \text{ and } N(x) = A \sigma(x)$$

which connects the axial force in the bar,  $N$ , to the resultant per unit length of the bond stresses on the perimeter of the bar,  $q$ . This equation has to be coupled with the constitutive laws for steel and bond, which can be expressed as

$$\sigma = \bar{\sigma}(\varepsilon(x)) = \bar{\sigma}\left(\frac{ds}{dx}\right) \quad \text{and} \quad \tau = \bar{\tau}(s(x)).$$

Note that here the influence of the deformation of concrete on slip has been considered negligible, as commonly assumed, and, as a consequence, the strain in the steel  $\varepsilon$  has been put equal to  $ds/dx$ .

Boundary values are specified at the two end points of the bar. Typically, for a pull-push displacement controlled test, the two displacements at the two ends are assigned; for a pull only test the boundary conditions are the value of the displacement at the pulled end and a null value of the axial force at the other end.

Different techniques can be used in principle for solving this nonlinear, two points boundary value problem: finite differences, finite elements, and shooting techniques. A finite element approach has been tried, for example, with some success in [5], using constant stress elements for the steel and concentrating bond forces (nonlinear springs) at the joints.

In this study a shooting technique has been preferred. It consists of transforming the boundary value problem into an initial value problem, in which the unknown boundary condition at one end has to be guessed, in order to produce, through integration along the length, the values of the normal force and the displacement at the other end. The given boundary condition at that end has now to be matched and this defines a nonlinear equation in the unknown boundary condition at the first end. This nonlinear equation is solved in this case using a modified secant method while the integration along the length is carried out using the trapezoidal scheme. The method has proved itself efficient and suitable for the problem at hand.

### 3.3 Behavior of Anchorages

Fig. 9 shows the calculated response of a main reinforcing bar (#8,  $d_p \sim 25$  mm) passing through a well-confined concrete ( $f'_c = 30$  N/mm<sup>2</sup>) of a column-beam joint having an anchorage length of  $15 d_p$ . It is loaded at one end only and subjected to reversed slip with increasing amplitude (Fig. 9a). The main aspects of this response, which are summarized below, agree well with those obtained in the experiments reported in [5].

- (a) The reduction in stiffness, characterized by pinched hysteretic loops, with increasing amplitude of displacement and number of cycles (Fig. 9c).
- (b) The reduction of strength at fixed amplitude of displacement as a function of the number of cycles (Fig. 9c).

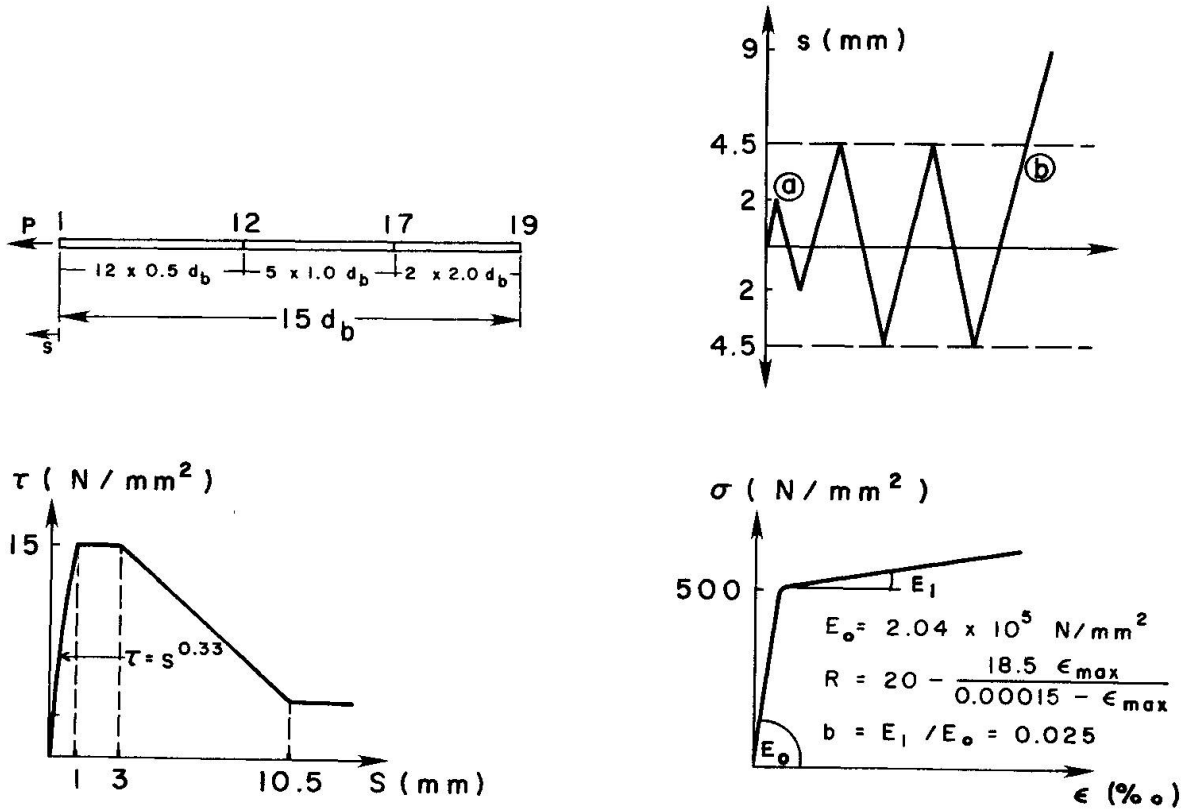


Fig. 9a Bar subdivisions, load history, local bond law and steel law.

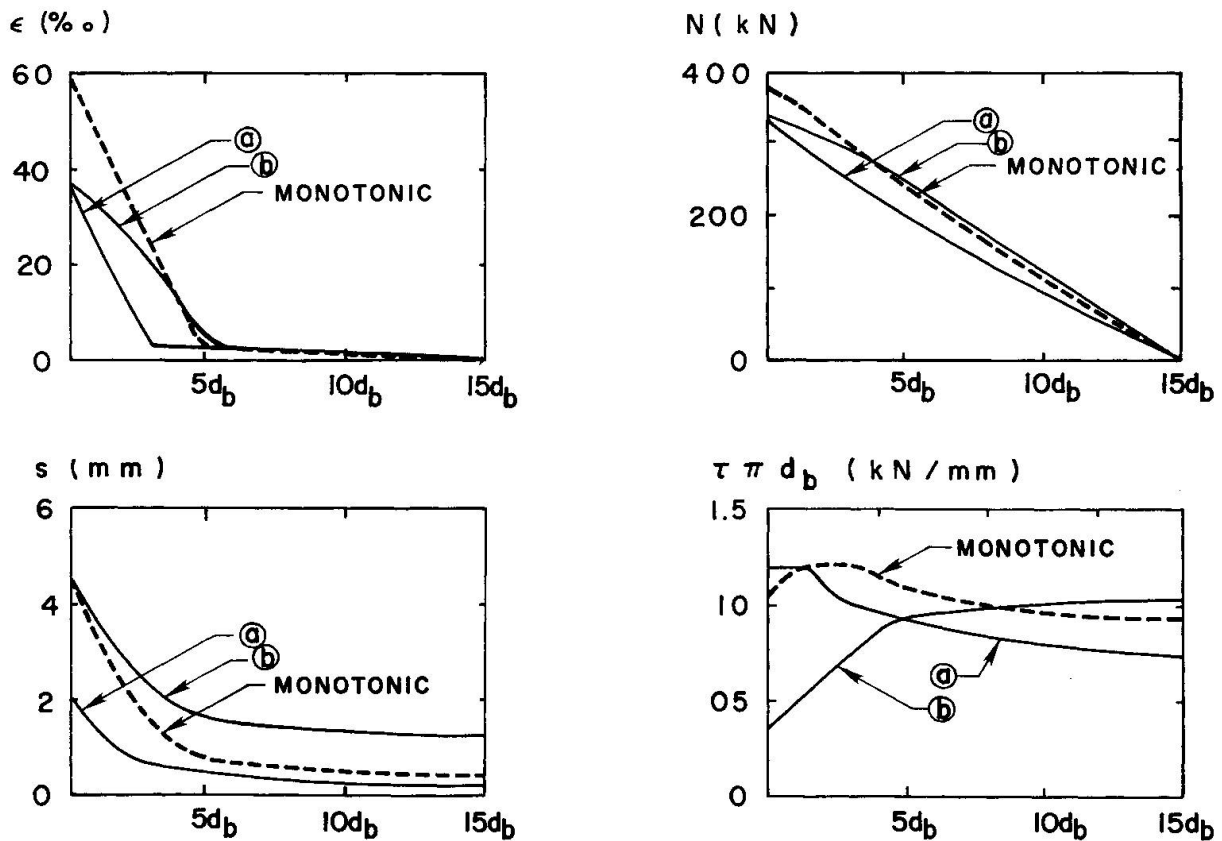


Fig. 9b Distribution of steel strain, slip, normal force and bond force along the bar at  $s = 2$  mm and  $s = 4.5$  mm for monotonic and cycling loading.

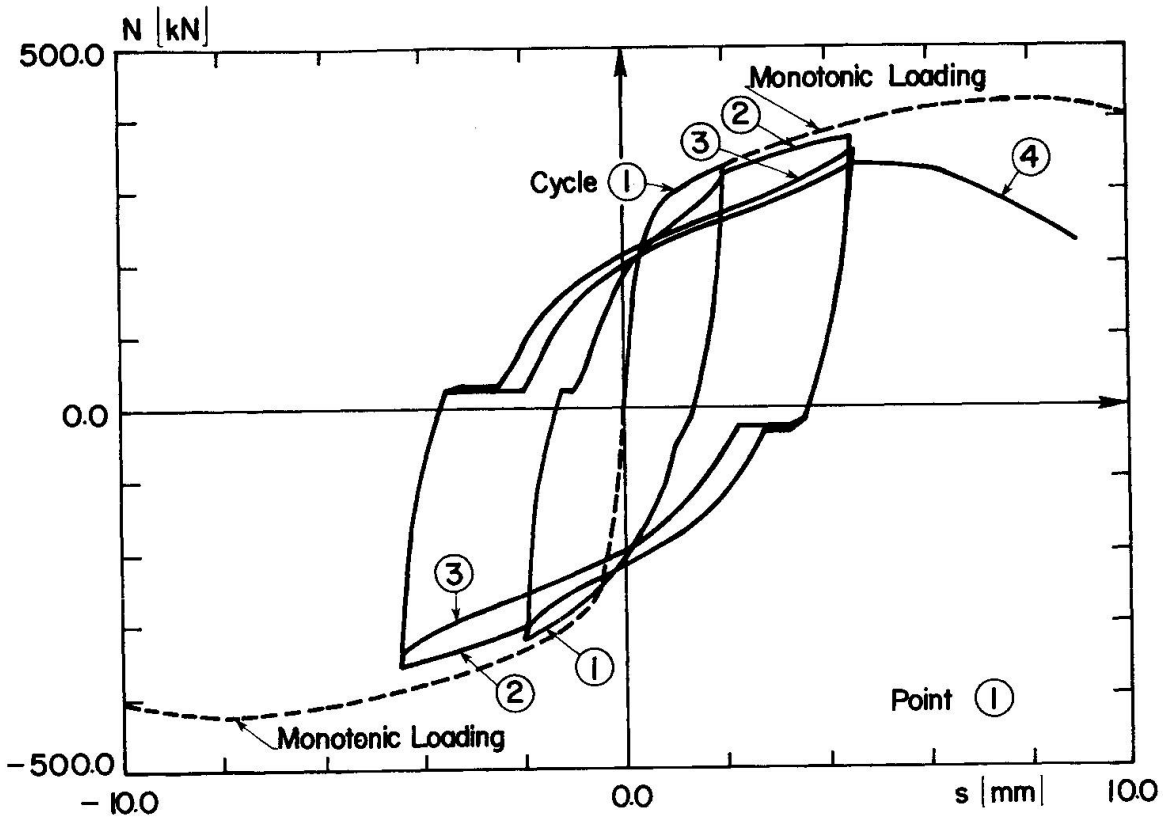


Fig. 9c Normal-force total slip relationship at loaded end.

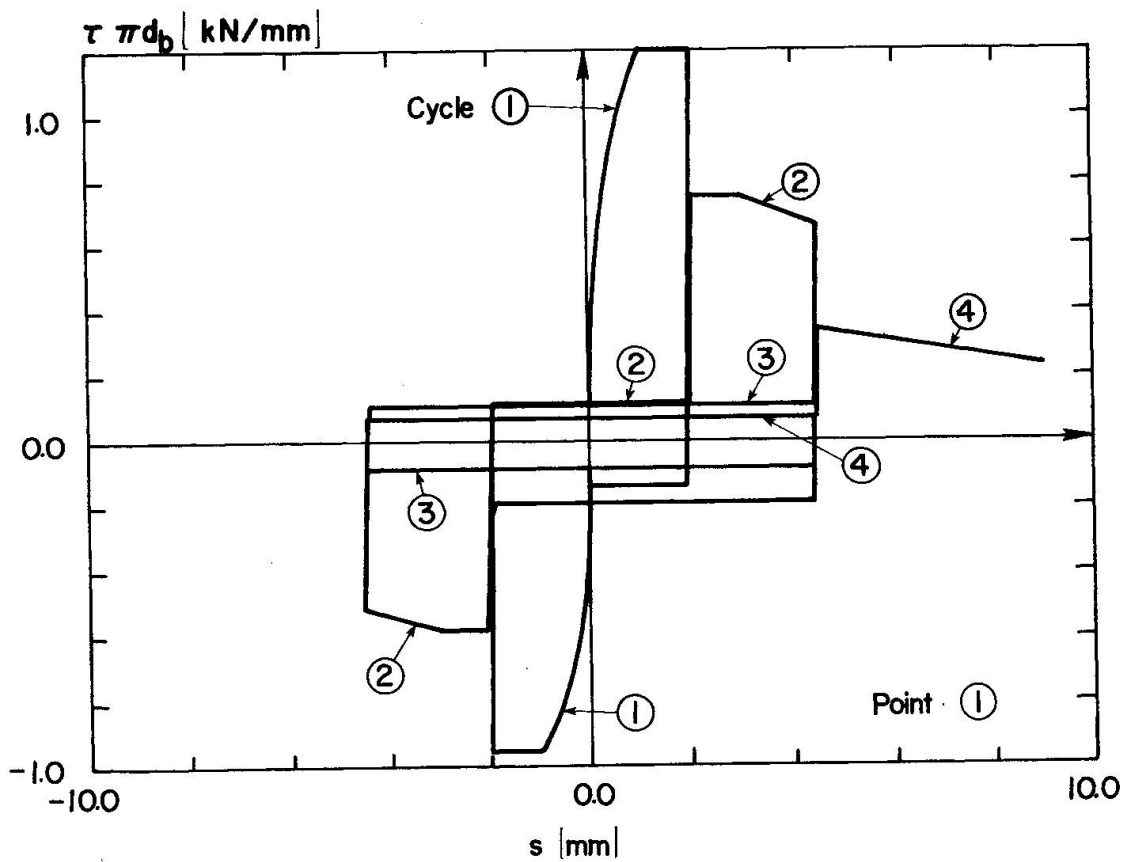


Fig. 9d Bond force-total slip relationship at loaded end.

Fig. 9 Analytically predicted behavior of the anchorage of a #8 deformed bar.



- (c) The reduction of maximum strength and of deformability at maximum strength (ductility) compared to monotonic loading (Fig. 9b,c).
- (d) The penetration of yield and the corresponding degradation of bond into the anchorage length with increasing peak displacement (see Figs. 9b,d).

However, the quantitative agreement between observed and calculated response needs improvement. Possible reasons for this discrepancy are given below:

- (a) In the present study it is assumed that the local bond stress-slip laws for tension and compression loading are equal and do not vary along the anchorage length. However, three different regions with significantly different bond stress-slip behaviors can be identified in a joint [5]: unconfined concrete in tension, confined concrete, and unconfined concrete in compression.
- (b) After yielding, the diameter of a bar in tension is significantly reduced due to the Poisson effect. This may reduce the bond resistance. The opposite is true for a bar yielding in compression. These effects were not taken into account.
- (c) The presented local bond stress-slip model might be over simplified in modeling the envelope curves (virgin and reduced) and particularly the ascending branches of the reloading curves near the peak slip, during and after cycling.

It is expected that after completing the next step of this current study in which the above mentioned effects will be taken into account, it should be possible to reproduce the experimental results with sufficient accuracy for practical applications.

#### 4. CONCLUSIONS

From the results obtained in this study the following main observations can be made:

- (1) During cycling loading the degradation of bond strength and bond stiffness depends primarily on the maximum value of peak slip in either direction reached previously. Other significant parameters are the number of cycles and the difference between the peak values of the slip between which the bar is cyclically loaded, i.e.,  $\Delta s = s_{\max} - s_{\min}$ .
- (2) Cycling up to 10 times between slip values corresponding to bond stresses smaller than approximately 80 percent of the maximum bond resistance,  $\tau_{\max}$ , attained under monotonically increasing slip, reduces moderately the bond resistance at the peak slip value as the number of cycles increase, but does not significantly affect the bond stress-slip behavior at larger slip values.
- (3) Cycling between slip limits larger than that corresponding to a bond stress of 80 percent of  $\tau_{\max}$  produces a pronounced deterioration of the bond stiffness at slip values smaller than the peak slip value and has a distinct effect on the bond stress-slip behavior at larger slip values.
- (4) The proposed model for the local bond stress-slip law is very simple compared with the real behavior but provides a satisfactory agreement with experimental results under various slip histories.



(5) While the calculated response of long anchorages of reinforcing bars agrees qualitatively well with experimental results, the quantification of the main parameters needs improvement. Reasons for the quantitative disagreement are given and are under study. It is expected that after introducing different local bond stress-slip relationships along the anchorage length, it will be possible to reproduce the experimental results with sufficient accuracy for practical applications.

#### ACKNOWLEDGEMENTS

The work reported herein was sponsored by the National Science Foundation, under grant PFR79-08984 with the University of California, Berkeley. The support of Dr. Ciampi by the Italian Research Council and of Dr. Eligehausen by the Deutsche Forschungsgemeinschaft are gratefully acknowledged.

#### REFERENCES

- [1] Popov, E. P., "Mechanical Characteristics and Bond of Reinforcing Steel under Seismic Conditions", Proceedings, Workshop on Earthquake-Resistant Reinforced Concrete Building Construction, University of California, Berkeley, July 11-15, Vol. II, pp. 658-682.
- [2] Takeda, T., Sozen, M., and Nielsen, N. N., "Reinforced Concrete Response to Simulated Earthquakes", *Journal of the Structural Division, ASCE*, Vol. 96, No. 12, Dec. 1970.
- [3] Ismail, M. A., and Jirsa, J. O., "Behavior of Enclosed Bars under Low Cycle Overloads Producing Inelastic Strains", *Journal of the American Concrete Institute*, Vol. 69, No. 7, July 1972.
- [4] Ma, S. Y., Bertero, V. V., and Popov, E. P., "Experimental and Analytical Studies on the Hysteretic Behavior of Reinforced Concrete Rectangular and T-Beams", Report No. EERC 76-2, Earthquake Engineering Research Center, University of California, Berkeley, 1976.
- [5] Viwathanatepa, S., Popov, E. P., and Bertero, V. V., "Effects of Generalized Loadings on Bond of Reinforcing Bars Embedded in Confined Concrete Blocks", Report No. EERC 79-22, Earthquake Engineering Research Center, University of California, Berkeley, 1979.
- [6] Tassios, T. P., "Properties of Bond between Concrete and Steel under Load Cycles Idealizing Seismic Actions", Bulletin D'Information No. 131 of the Comité Euro-International du Béton, Paris, April 1979.
- [7] Eligehausen, R., Bertero, V. V. and Popov, E. P., "Local Bond Stress-Slip Relationships of Deformed Bars under General Excitations", Report in preparation - UCB.
- [8] Rehm, G., "Über die Grundlagen des Verbundes zwischen Stahl und Beton", (About the Basic Laws of Bond between Steel and Concrete), Schriftenreihe des Deutschen Ausschusses für Stahlbeton, Berlin, 1961.
- [9] Bresler, B. and Bertero, V. V., "Behavior of Reinforced Concrete Under Repeated Loads", *Journal of the Structural Division, ASCE*, Vol. 24, No. 6, June 1968.



- [10] Ismail, M. A. and Jirsa, J. O., "Bond Deterioration in Reinforced Concrete Subject to Low Cycle Loads", Journal of the American Concrete Institute, June 1972.
- [11] Morita, S., and Kaku, T., "Local Bond Stress-Slip Relationship and Repeated Loading", IABSE Symposium, Resistance and Ultimate Deformability of Structures Acted on by Well-Defined Repeated Loads, Lisbon, 1973.
- [12] Rehm, G., and Eligehausen, R., "Einfluss einer nicht ruhenden Belastung auf das Verbundverhalten von Rippenstählen", (Influence of High Cycle Repeated Loads on the Bond Behavior of Ribbed Reinforcing Bars), Betonwerk und Fertigteil-Technik, Heft 6, 1977, in German.
- [13] Giuffré, A. and Pinto, P. E., "Reinforced Concrete Behavior under Strong Repeated Loading", G. Genio Civile, No. 5, 1970, in Italian.
- [14] Capecchi, D., Ciampi, V., and Vestroni, "Numerical Studies on the Behavior of a Reinforced Concrete Beam Element under Repeated Loadings", Bulletin D'Information No. 132 of the Comité Euro-International du Béton, Paris, April 1979.
- [15] Jennings, P. C., "Response of Simply Yielding Structures to Earthquake Excitation", California Institute of Technology, Pasadena, Californiam Report No. 6360, June 1963.



Leere Seite  
Blank page  
Page vide